Title

Up-gradient particle flux in a drift wave-zonal flow system

Journal

Physics of Plasmas, 22(5)

ISSN

1070-664X

Authors

Cui, L
Tynan, GR
Diamond, PH
et al.

Publication Date

2015-05-01

DOI

10.1063/1.4921671

Up-gradient particle flux in a drift wave-zonal flow system

L. Cui, G. R. Tynan, P. H. Diamond, S. C. Thakur, and C. Brandt

Citation: Physics of Plasmas (1994-present) **22**, 050704 (2015); doi: 10.1063/1.4921671
View online: http://dx.doi.org/10.1063/1.4921671
View Table of Contents: http://scitation.aip.org/content/aip/journal/pop/22/5?ver=pdfcov
Published by the AIP Publishing

Up-gradient particle flux in a drift wave-zonal flow system

L. Cui,[1,2] G. R. Tynan,[1,2] P. H. Diamond,[1,3] S. C. Thakur,[1,2] and C. Brandt[2]
[1]*Center for Momentum Transport and Flow Organization, UC San Diego, La Jolla, California 92093, USA*
[2]*Center for Energy Research, UC San Diego, La Jolla, California 92093, USA*
[3]*Center for Astrophysics and Space Sciences (CASS) and Department of Physics, UC San Diego, La Jolla, California 92093, USA*

(Received 12 January 2015; accepted 17 April 2015; published online 20 May 2015)

We report a *net inward, up-gradient* turbulent particle flux in a cylindrical plasma when collisional drift waves generate a sufficiently strong sheared azimuthal flow that drives positive (negative) density fluctuations up (down) the background density gradient, resulting in a steepening of the mean density gradient. The results show the existence of a saturation mechanism for drift-turbulence driven sheared flows that can cause up-gradient particle transport and density profile steepening. [http://dx.doi.org/10.1063/1.4921671]

Up-gradient transport processes play a critical role in maintaining non-equilibrium conditions across a wide-range of systems. For example, in eukaryote cells, transport of Na^+/K^+ ions across the cell membrane occurs via the hydrolysis of the ATPase molecule that releases chemical potential energy, which drives a molecular motor that then does work on the Na^+/K^+ ions and moves them across the membrane up their concentration gradient.[1] In open fluid thermodynamic systems that are driven out of equilibrium by heat input, up-gradient transport can occur as in, e.g., the convective planetary boundary layer[2] and in carefully constructed experimental systems.[3] In magnetically confined plasmas, up-gradient transport mechanisms have been invoked to explain the observed time-averaged plasma density and temperature profiles in astrophysical and near-Earth space plasmas[4–9] and in controlled fusion confinement experiments.[10–15]

For fusion systems, inferred transport fluxes are often decomposed into an inward-directed turbulent pinch and down-gradient diffusive transport components (both of which are attributed to a combination of density and temperature gradients) that then compete to form the plasma equilibrium. In a few cases, direct measurements of net inward turbulent particle fluxes have been reported during or shortly after the formation of transport barriers associated with the formation of a suitably strong $E \times B$ shear layer[16–19] or during the application of an externally forced $E \times B$ shear flow.[20] However, the cause of the net inward flux in these latter works was never identified, nor has velocity shear ever been considered as a possible mechanism to drive inward pinches in confinement experiments. In this paper, we show that *net inward, up-gradient* turbulent particle fluxes in a magnetized plasma are caused by the radially sheared azimuthal flow which drives the turbulent flux up the gradient.

Our previous studies have shown that at moderate magnetic fields the plasma develops coherent, finite amplitude collisional drift wave fluctuations in the region around the density gradient maximum. As the magnetic field is increased further, the plasma develops two velocity shear layers that sit on either side of the density gradient maximum.[21,22] At the outer shear layer, the turbulent stress does work on and sustains the shear flow against dissipation, consistent with earlier results[23–30] and under some conditions, in the region between the maximum density gradient and outer shear layer, a net inward flux is observed.[21]

The critical new finding reported here is the identification of the role that velocity shear plays in driving this up-gradient transport. In particular, we find that when and where this up-gradient flux occurs, the sheared flow does work on the fluctuations that are responsible for the up-gradient flux. The bulk (80%) of the up-gradient flux is carried by large amplitude (exceeding one standard deviation) positive (negative) density perturbations that move up (down) the density gradient. Correlation studies show that a transient increase (decrease) in the shear flow results in a subsequent increase (decrease) in the inward flux, demonstrating the causal relationship between flow shear and up-gradient flux. Finally, when the up-gradient flux occurs, the time-averaged density profile steepens. It is particularly remarkable that these observations are made in a simple plasma system described by the Hasegawa-Wakatani model of the drift turbulence-zonal flow system. Clearly then drift turbulence not only can generate a sheared flow that acts to regulate the rate of cross-field transport,[31] but under some conditions the shear flow can be a source of turbulence that surprisingly can cause an up-gradient particle flux that enhances the density gradient. Thereby a new feedback loop is formed in the regulation of time-averaged density and velocity gradients by the coupled drift turbulence-sheared flow system.

This experiment was carried out on the upgraded CSDX linear helicon plasma device, which is 2.8 m long operating with 1.8 kW rf power input and a gas fill pressure of 3.2 mTorr. A high-speed (210 526 frames/s) camera is placed at the end of the machine to capture the dynamics of propagating structures seen in the plasma visible light emission.[21,32] Measurements of mean plasma profiles and the fluctuating density, potential, and the resulting turbulent particle flux are made by an 18-tip Langmuir probe and a 4-tip Langmuir

probe at two axial port positions separated by 75 cm. Details about the layouts of the two probes can be found in Refs. 33 and 34. Both probe systems have shown similar experimental results and, in particular, shown similar inward fluxes.

Radially resolved profiles with 1 mm spatial resolution/100 ms duration time averages for several different magnetic fields are shown in Fig. 1. Heat input from the RF source sustains a centrally peaked plasma density [Fig. 1(a)] and electron temperature profile[21] (not shown here). The density profile becomes steeper at $r = 2.5$ cm as we increase the magnetic field to 1200 G. Fig. 1(b) shows the radial profiles of the time-averaged azimuthal velocity computed using a time-delay estimate (TDE) technique applied to imaging data. A radially sheared azimuthal flow in the ion diamagnetic drift direction is observed near the center of the plasma for $r < 2$ cm (denoted as the inner shear layer) and another azimuthally symmetric sheared flow (denoted the outer shear layer) in the electron drift direction located at $r \sim 6$ cm develops as we increase the magnetic field. The density gradient maximum is located between the two shear layers, and the flow approximates solid body rotation in that the azimuthal velocity increases linearly with distance. The onset of fluctuation-driven net inward (i.e., up the density gradient) particle flux $\langle \tilde{n}\tilde{V}_r \rangle$ [Fig. 1(c)] starts when both the strength of the outer shear layer becomes sufficiently strong ($B \geq 1100$ G) and the inner shear layer begins to develop. This steepening is to be expected since the total particle loss rate due to radial transport is comparable to loss of particles due to parallel plasma flow to the ends of the device. Therefore, the up-gradient particle transport must be driven by some new mechanism that drives the fluctuations against the gradient; the shear flow naturally then emerges as a possible candidate.

In order to determine if there is a link between the shear flow and up-gradient flux, we examine the rate of work done on the flow by the turbulence, which is given by the Reynolds work $-\frac{\partial \langle \tilde{V}_r \tilde{V}_\theta \rangle}{\partial r} \langle \bar{V}_\theta \rangle$. Here, a positive value of

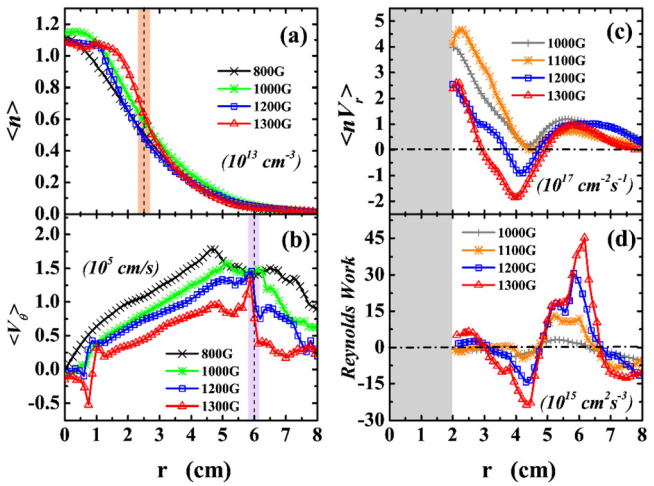

FIG. 1. Time-averaged radial profiles of (a) mean density $\langle n_o \rangle$, (b) mean azimuthal velocity $\langle \bar{V}_\theta \rangle$, (c) turbulent particle flux $\langle \tilde{n}\tilde{V}_r \rangle$, and (d) mean total Reynolds work $-\frac{\partial \langle \tilde{V}_r \tilde{V}_\theta \rangle}{\partial r} \langle \bar{V}_\theta \rangle$. (c) and (d) show the data from the 18-tip probe, which is only available for $r > 2$ cm since the probe tips start arcing and overheat when they get too close to the core plasma.

Reynolds work indicates that the fluctuations are driving the shear flow, while a negative value shows the fluctuations are extracting kinetic energy from the flow. An examination of the radial profile of the Reynolds work provides a key insight into the origin of the inward particle flux. As shown in Fig. 1(d), at the outer shear layer region $5 < r < 6.5$ cm, the fluctuations do work on the shear flow and sustain it against dissipation as shown in earlier work.[23,35] For $B > 1100$ G, in the region $3 < r < 5$ cm where the inward turbulent particle flux is observed the Reynolds work is negative, indicating that here the shear flow is driving the higher frequency fluctuations. Thus, the up-gradient flux occurs when and where the shear flow drives the fluctuations.

This inward flux is also observed with other diagnostics. In Fig. 2(a), we plot the cross-correlation coefficient computed between the Langmuir probe ion saturation current I_{sat} and the camera fluctuating visible light intensity I_c. The results show that $Corr(I_{sat}, I_c)$ reaches values as large as 0.75 with a zero delay time. Thus, the light intensity fluctuations are associated with plasma density fluctuations. Motivated by this fact, we have taken time-resolved movies of the motion of turbulent density perturbations (archived in Ref. 21) to identify turbulent structure motion over a sequence of frames. This motion can then be used to construct a velocity field and streamlines associated with the turbulent light intensity structure motion (essentially equivalent to the motion of turbulent density structures). The results [Fig. 2(b)] reveal that at $B = 1000$ G, positive density structures anywhere in the plasma cross-section tend to spiral radially outward and move azimuthally in the electron diamagnetic drift direction. The net result is an outward flux of light intensity (and thus of density) across the plasma column. In contrast, the velocity field at $B = 1300$ G [Fig. 2(c)] shows a very different behavior. We find that streamlines launched from the region exhibiting a net inward particle flux (blue dot in Fig. 2(c)) *spiral inwards*. This inward motion stops at a closed surface located at $r \sim 2$ cm, forming an effective barrier through which the fluctuations do not penetrate [Fig. 2(c)]. At radii $r > 4$–5 cm, the velocity field is dominated by radial-azimuthal outward spirals, indicative of outward transport that is consistent with the observations of outward particle flux in the outer region of the plasma as seen in the probe data. To further confirm this inward particle transport, we plot the corresponding intensity flux $\langle \tilde{I}_c \tilde{V}_r \rangle$ from the movies for $B = 1000$ G and 1300 G [Fig. 2(d)]. Here, I_c denotes the deviation of the instantaneous light intensity from the time-averaged value at a given location, and $\tilde{V}_r$ denotes the radial component of the fluctuating velocity of this light intensity fluctuation inferred from the velocimetry analysis described above. The result (Fig. 2(d)) shows that the radial flux of the fluctuating light intensity—which is proportional to the radial particle flux—exhibits the same inward flux phenomena found above in the Langmuir probe measurements at $B = 1300$ G. Thus, two independent diagnostic measurements confirm the existence of an inward flux at ~1300 G. We note that at lower magnetic fields, the probe and imaging do not show a strong agreement. This might be due to the finite $k_\parallel$ of drift waves which dominate the fluctuations at 1000 G, and the fact that there is a Kelvin-Helmholtz

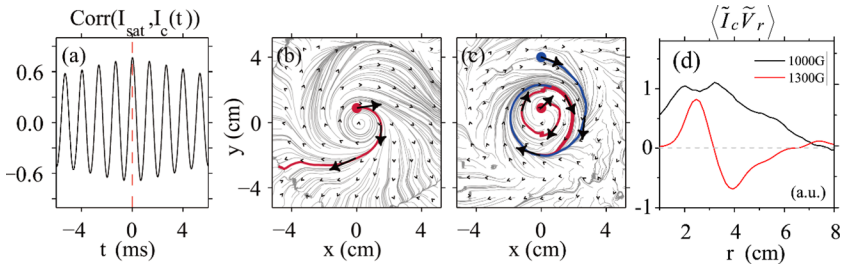

FIG. 2. (a) Cross-correlation coefficient between the Langmuir probe and the fast camera signals. (b) and (c) Frequency averaged velocity fields obtained from velocimetry of the camera movies shown in streamline plots at B = 1000 G (b) and 1300 G (c). The direction of the magnetic field is ⊗. (d) Evolution of Intensity flux $\langle \tilde{I}_c \tilde{V}_r \rangle$.

instability (which has $k_\parallel = 0$) at higher B field. As a result, we have $\frac{k_\parallel}{k_\perp}|_{1300G} < \frac{k_\parallel}{k_\perp}|_{1000G}$. Since the camera integrates the light intensity over a depth-of-field of $\delta z \sim 10$ cm. At the lower magnetic field, the helical nature of the fluctuations will then cause them to be partially blurred, which will in turn begin to cause difficulties with inferring the intensity flux $\langle \tilde{I}_c \tilde{V}_r \rangle$. However, this conjecture needs to be explored in future work. Regardless of this issue, it is clear that for 1300 G conditions, two independent diagnostic techniques see the development of an inward particle flux and the mean density gradient steepens in response to this inward flux.

Further insight can be obtained by performing a conditional average analysis of the probe data. When the instantaneous fluctuating positive density excursion $\tilde{n}$ exceeds one standard deviation σ_n at time τ, a positive density fluctuation event is considered to have been triggered. Similarly, negative density fluctuation events are identified when a negative density excursion exceeding one negative standard deviation $-\sigma_n$ occurs. We record the fluctuating azimuthal electric field of each event, and then compute the radial profile of the average effective radial E × B propagation velocity V_r^{eff} for both positive and negative fluctuation events. The results are shown in Fig. 3(b) for B = 1300 G. We observe across the region of $3 < r < 5$ cm that *positive density fluctuations propagate inwards*, against the density gradient, while *negative density fluctuations propagate outwards*, down the density gradient. In this region, the total net fluctuation-driven particle flux [red dashed line in Fig. 3(c)] is negative where the shear flow drives the fluctuations [Fig. 3(a)]. This structure motion is opposite to the expectation for blob/hole dynamics associated with density gradient relaxation.[36] The flux carried by density fluctuations with amplitudes larger than one standard deviation is ~80% of the total fluctuation-driven flux [Fig. 3(c)]. Clearly then the inward flux is associated with some different driving force that affects the dynamics of turbulent structures in the intermediate region.

The above results show a correlation between the shear flow and the inward particle flux. To test if there is a causal link between flow shear and inward flux, we compute the cross-correlation between fluctuations in the shearing rate and particle flux, Corr $(\bar{V}'_\theta, \Gamma_{particle})$, at $r = 4.8$ cm, which is the outermost region of up-gradient flux. Here, the time varying instantaneous shearing rate is determined by time-delay estimation analysis of the same probe data used to find the particle flux. The result [Fig. 4(a)] shows that the velocity shearing rate and particle flux do have a significant correlation (peak correlation of ~0.4, well above the noise level of ~0.1) with a finite time delay (~18 μs). The width of the

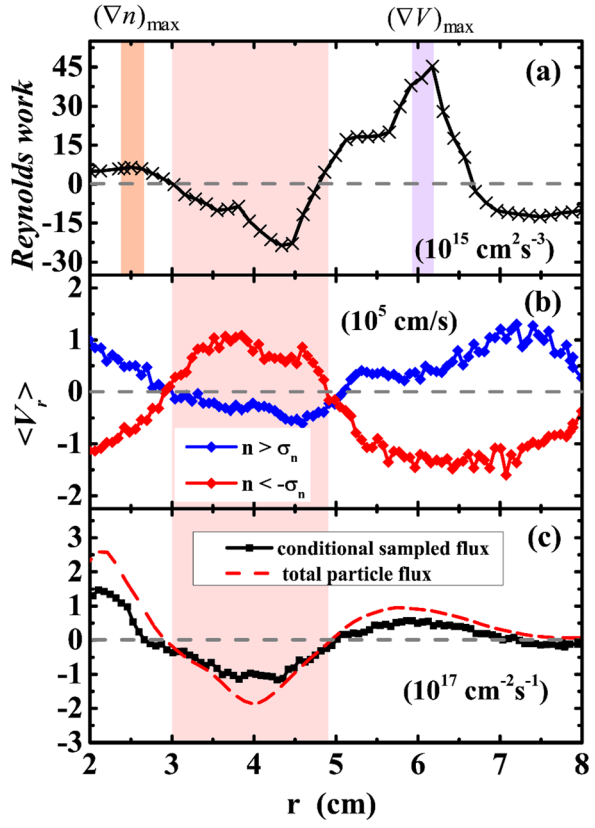

FIG. 3. B = 1300 G: (a) Radial profile of mean total Reynolds work. (b) Radial velocity profiles for positive density fluctuation events (blue solid diamond) and negative density fluctuation events (red solid diamond). (c) The sum of contribution of density fluctuation events with amplitudes larger than one standard deviation to the particle flux (black solid squares) and total particle flux (red dashed line).

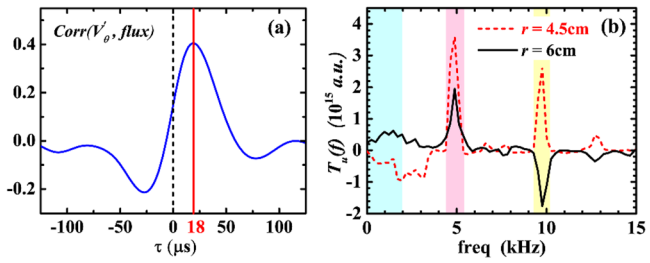

FIG. 4. B = 1300 G: (a) Cross-correlation between azimuthal velocity shearing rate and turbulent particle flux at r = 4.8 cm. An increase in azimuthal shearing rate leads to a subsequent increase in the inward turbulent particle flux ~18 μs later. (b) Total net kinetic energy transfer rate $T_u(f)$ at $r = 4.5$ cm (red dashed line) and $r = 6$ cm (black solid line). Here, a negative value of T_u means that frequency f is losing energy and a positive value means that it is gaining energy.

envelope of correlation function, which corresponds to the decorrelation time of the flow, is about 0.3 ms that consistent with the time-scale of the fluctuations associated with the up-gradient particle flux. These results clearly indicate that a transient increase in the local azimuthal shearing rate is *followed* by a subsequent increase in the inward-directed fluctuation-driven particle flux, demonstrating that a causal relationship exists between the velocity shear and up-gradient particle flux.

We can gain additional insight into the relationship between the fluctuations responsible for the inward flux and the shear flow by examining the nonlinear transfer of kinetic energy in the frequency domain. From the frequency-resolved flux Γ_{turb} profiles,[37] we observe that both the inward flux at r = 4.5 cm and outward flux at $r = 6$ cm are due primarily to fluctuations at frequency $f \sim 5$ kHz. We then calculate the net nonlinear kinetic energy transfer $T_u(f) = \sum_{f_1} T_u(f, f_1)$, where $T_u(f, f_1) = -R_e\langle \tilde{u}_f^* \cdot (\tilde{u}_{f_2} \cdot \nabla)\tilde{u}_{f_1} \rangle$ with $f_2 = f - f_1$ and $\tilde{u}_f$ denotes the Fourier-transformed fluctuating E × B velocity estimated from the probe array. A positive (negative) value for $T_u(f)$ indicates the kinetic energy is being nonlinearly transferred into (out of) the frequency f via interactions across a range of frequencies f_1. A detailed discussion of the probe arrays used for this measurement and the interpretation of the results is available in the literature.[34] Examining $T_u(f)$ [Fig. 4(b)], we find that at $r = 6$ cm, where the shearing rate is largest, the low-frequency flows are gaining energy from the higher frequency fluctuations, consistent with the expectations for a turbulence-driven zonal flow. However, at $r = 4.5$ cm, where the net particle flux is negative, the f ∼ 5 kHz fluctuations which are responsible for the inward particle flux are *gaining energy* from the low frequency ($f <$ 1–2 kHz) sheared flow. This provides yet an additional piece of evidence linking the shear flow to the generation of the inward, up-gradient particle flux.

The experimental findings listed above can be summarized with the schematic shown in Fig. 5. The black portion of the schematic presents the classic paradigm of drift wave-zonal flow turbulence energetics and saturation.[35] A mean density gradient ∇n can drive collisional drift wave turbulence that causes an outward turbulent particle flux, which flattens the density gradient. A finite turbulence-driven Reynolds stress in turn can amplify the shear flow by doing positive Reynolds work on it. This results in a feedback loop that leads to down-gradient turbulent flux and shear flow saturation set by the linear drive associated with the free energy source, the high-k dissipation rate of the turbulence, and the (presumably linear) damping rate of the shear flow. The results here show that, at least under some conditions, a new feedback loop can develop as shown by the red portion of Fig. 5. In particular, the results indicate that the sheared flow ∇v can perform work on the fluctuations (presumably by some to-be-identified shear layer-turbulent structure interaction). A similar picture of an anomalous shear flow damping was presented in Ref. 35 and was also found in gyrokinetic simulations.[38] Surprisingly, our results show that this then can lead to an up-gradient particle flux which steepens the density gradient. As a result, the system becomes self-regulated by diffusive outward particle transport caused by drift wave turbulence and non-diffusive inward particle transport driven by flow.

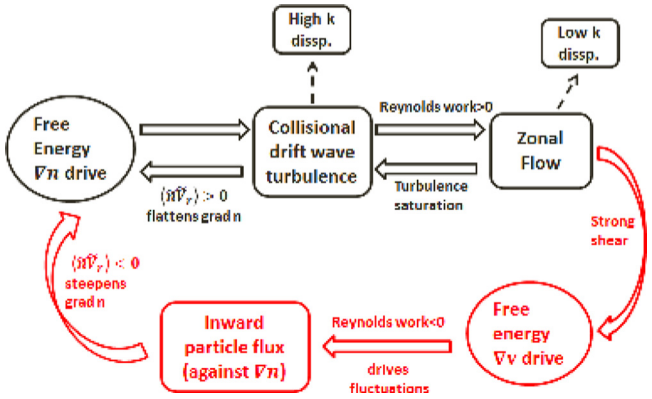

FIG. 5. A self-regulating feedback loop of DWT-ZF system with multiple free energy sources. Black route: classic ∇n-driving drift wave-zonal flow turbulence. Red route: feedback loop due to free energy source ∇v.

It is of course well known that a background flow shear with an inflection point can act as a free-energy source of fluctuations via the linear Kelvin-Helmholtz (KH) instability.[11] Therefore, one is tempted to invoke a simple localized linear KH instability. However, two observations weigh against interpreting the up-gradient flux in terms of a simple local linear KH. First, the region of localized linear KH instability (r > 5.5 cm) lies outside the region of up-gradient flux.[21] Second, we have shown that the fluctuations responsible for the up-gradient flux are *nonlinearly* driven by the shear flow. In particular, this nonlinear drive occurs as a result of the phase coherence between variations in the shearing rate, the radial-azimuthal motion of turbulent structures, and the density fluctuations. Otherwise the cross-bispectrum [Fig. 4(b)] and the correlation [Fig. 4(a)] would both vanish. However, a complete study of the global linear stability of the system using experimental profiles is needed. Further work is also required to determine if parallel flow plays any role in generating up-gradient particle fluxes. Both of these topics are under study and will be presented in future publications.

As noted earlier, tokamak experiments have sometimes shown evidence for an inward turbulent flux that are usually coincident with strong edge pressure gradients and E × B shear flows found in improved confinement regimes[16–19] and space plasma observations also indicate up-gradient transport processes with simultaneous density gradient and E × B shear regions.[4–8] These earlier observations are reminiscent of the results reported here, suggesting similar mechanisms could be at work in both cases (although theory shows magnetic shear to be effective at quenching the linear transverse KH instability[39]). Thus, theory that considers flow shear as an additional spatially separated free energy source that can drive particle flux in systems with weak or vanishing magnetic shear should therefore be developed and applied to these observations.

This work was supported by the U.S. Department of Energy through Grant No. DE- SC0001961. The authors also acknowledge the useful discussions with R. Singh.

[1]J. H. Kaplan, Annu. Rev. Biochem. **71**, 511 (2002).
[2]A. A. M. Holtslag and C. H. Moeng, J. Atmos. Sci. **48**, 1690 (1991).
[3]P. Urban, D. Schmoranzer, P. Hanzelka, K. R. Sreenivasan, and L. Skrbek, Proc. Natl. Acad. Sci. U.S.A. **110**, 8036 (2013).
[4]C. G. Falthammar, J. Geophys. Res. **70**, 2503, doi:10.1029/JZ070i011p02503 (1965).
[5]T. J. Birmingh, J. Geophys. Res. **74**, 2169, doi:10.1029/JA074i009p02169 (1969).
[6]J. G. Lyon, Science **288**, 1987 (2000).
[7]A. C. Boxer, R. Bergmann, J. L. Ellsworth, D. T. Garnier, J. Kesner, M. E. Mauel, and P. Woskov, Nat. Phys. **6**, 207 (2010).
[8]M. Schulz and L. J. Lanzerotti, *Particle Diffusion in the Radiation Belts* (Springer-Verlag, 1974).
[9]T. A. Farley, A. D. Tomassian, and M. Walt, Phys. Rev. Lett. **25**, 47 (1970).
[10]F. Wagner and U. Stroth, Plasma Phys. Controlled Fusion **35**, 1321 (1993).
[11]X. Garbet, L. Garzotti, P. Mantica, H. Nordman, M. Valovic, H. Weisen, and C. Angioni, Phys. Rev. Lett. **91**, 035001 (2003).
[12]G. T. Hoang, C. Bourdelle, X. Garbet, J. F. Artaud, V. Basiuk, J. Bucalossi, F. Clairet, C. Fenzi-Bonizec, C. Gil, J. L. Segui *et al.*, Phys. Rev. Lett. **93**, 135003 (2004).
[13]C. Bourdelle, Plasma Phys. Controlled Fusion **47**, A317 (2005).
[14]J. Weiland, A. Eriksson, H. Nordman, and A. Zagorodny, Plasma Phys. Controlled Fusion **49**, A45 (2007).
[15]D. R. Baker, "A perturbation solution to the drift kinetic equation yields pinch type fluxes from the circulating electrons," presented at the Transport Task Force Workshop, Madison, 2003.
[16]S. H. Muller, J. A. Boedo, K. H. Burrell, J. S. deGrassie, R. A. Moyer, D. L. Rudakov, W. M. Solomon, and G. R. Tynan, Phys. Plasmas **18**, 072504 (2011).
[17]J. Boedo, D. Gray, R. Conn, S. Jachmich, G. Van Oost, and R. R. Weynants, Czech. J. Phys. **48**, 99 (1988).
[18]M. G. Shats and D. L. Rudakov, Phys. Rev. Lett. **79**, 2690 (1997).
[19]U. Stroth, T. Geist, J. P. T. Koponen, H. J. Hartfuss, P. Zeiler, and ECRH and W7-AS Team, Phys. Rev. Lett. **82**, 928 (1999).
[20]T. A. Carter and J. E. Maggs, Phys Plasmas **16**, 012304 (2009).
[21]S. C. Thakur, C. Brandt, L. Cui, J. J. Gosselin, A. D. Light, and G. R. Tynan, Plasma Sources Sci. Technol. **23**, 044006 (2014).
[22]M. J. Burin, G. R. Tynan, G. Y. Antar, N. A. Crocker, and C. Holland, Phys. Plasmas **12**, 052320 (2005).
[23]C. Holland, J. H. Yu, A. James, D. Nishijima, M. Shimada, N. Taheri, and G. R. Tynan, Phys. Rev. Lett. **96**, 195002 (2006).
[24]Z. Yan, M. Xu, P. H. Diamond, C. Holland, S. H. Muller, G. R. Tynan, and J. H. Yu, Phys. Rev. Lett. **104**, 065002 (2010).
[25]M. Xu, G. R. Tynan, P. H. Diamond, C. Holland, J. H. Yu, and Z. Yan, Phys. Rev. Lett. **107**, 055003 (2011).
[26]M. Xu, G. R. Tynan, C. Holland, Z. Yan, S. H. Muller, and J. H. Yu, Phys. Plasmas **17**, 032311 (2010).
[27]G. R. Tynan, C. Holland, J. H. Yu, A. James, D. Nishijima, M. Shimada, and N. Taheri, Plasma Phys. Controlled Fusion **48**, S51 (2006).
[28]C. Holland, G. R. Tynan, J. H. Y. A. James, D. Nishijima, M. Shimada, and N. Taheri, Plasma Phys. Controlled Fusion **49**, A109 (2007).
[29]Z. Yan, G. R. Tynan, C. Holland, M. Xu, S. H. Muller, and J. H. Yu, Phys. Plasmas **17**, 012302 (2010).
[30]Z. Yan, G. R. Tynan, C. Holland, M. Xu, S. H. Muller, and J. H. Yu, Phys. Plasmas **17**, 032302 (2010).
[31]A. Hasegawa and M. Wakatani, Phys. Rev. Lett. **59**, 1581 (1987).
[32]A. D. Light, S. C. Thakur, C. Brandt, Y. Sechrest, G. R. Tynan, and T. Munsat, Phys. Plasmas **20**, 082120 (2013).
[33]Z. Yan, J. H. Yu, C. Holland, M. Xu, S. H. Muller, and G. R. Tynan, Phys. Plasmas **15**, 092309 (2008).
[34]M. Xu, G. R. Tynan, C. Holland, Z. Yan, S. H. Muller, and J. H. Yu, Phys Plasmas **16**, 042312 (2009).
[35]P. H. Diamond, S. I. Itoh, K. Itoh, and T. S. Hahm, Plasma Phys. Controlled Fusion **47**, R35 (2005).
[36]J. A. Boedo, D. Rudakov, R. Moyer, S. Krasheninnikov, D. Whyte, G. McKee, G. R. Tynan, M. Schaffer, P. Stangeby, P. West *et al.*, Phys. Plasmas **8**, 4826 (2001).
[37]See supplementary material at http://dx.doi.org/10.1063/1.4921671 for frequency-resolved particle flux profiles for B = 1300 G.
[38]B. N. Rogers, W. Dorland, and M. Kotschenreuther, Phys. Rev. Lett. **85**, 5336 (2000).
[39]T. Chiueh, P. W. Terry, P. H. Diamond, and J. E. Sedlak, Phys. Fluids **29**, 231 (1986).